CHAPTER II

LITERATURE REVIEW

2.1 Overview of Titanium dioxide

Titanium dioxide (TiO_2) is one of the most popular ceramic materials with a large number of applications. It is generally used as a white pigment or opacifier, enameling, gas sensor, cosmetic, as well as a photocatalyst [1]. In natural, TiO_2 exists in three polymorphs. Two tetragonal forms are anatase and rutile. Another orthorhombic form is brookite. Since brookite is extremely difficult to synthesize in the laboratory, only anatase and rutile are commercially important.

Typically, anatase is the initial form of product in inorganic synthesis. It has been reported that anatase phase is metastable form and converts to rutile at elevated temperature. The transformation is exothermic. Meanwhile, rutile is the thermodynamically stable phase. Both anatase and rutile have a tetragonal crystal structure consisting of the chains of TiO_6^{2-} octahedron. Previous reports suggested that it normally existed as a six-fold coordinated $[Ti (H_2O)_6]^{4+}$ complex. The two structures are different in the distortion of each octahedral. Figure 2.1 shows the bulk structure of anatase and rutile. Each Ti^{4+} ion is surrounded by the six O^{2-} ions forming octahedron. The octahedra in anatase and rutile are not regular. They slightly distort. The Ti-Ti distances of anatase are 3.782 and 3.04 Å, whereas those of rutile are 3.57 and 2.953 Å. These show that the Ti-Ti distances of anatase are longer than that of rutile. The Ti-O distances of anatase are 1.937 and 1.966 Å while those of rutile are 1.946 and 1.983 Å, indicating the Ti-O distances of anatase are shorter than those of rutile. In anatase structure each octahedron is in contact with eight neighboring octahedrons, sharing four edge oxygen pairs and four corner oxygen atoms. Unlike in rutile structure, each octahedron is in contact with ten neighboring octahedrons,

sharing two edges and eight corners. The mismatch in their structure leads to having different mass density and electronic band structure, as indicated in Table 2.1.

Table 2.1 The crystal structure and physical properties of TiO_2 [8]

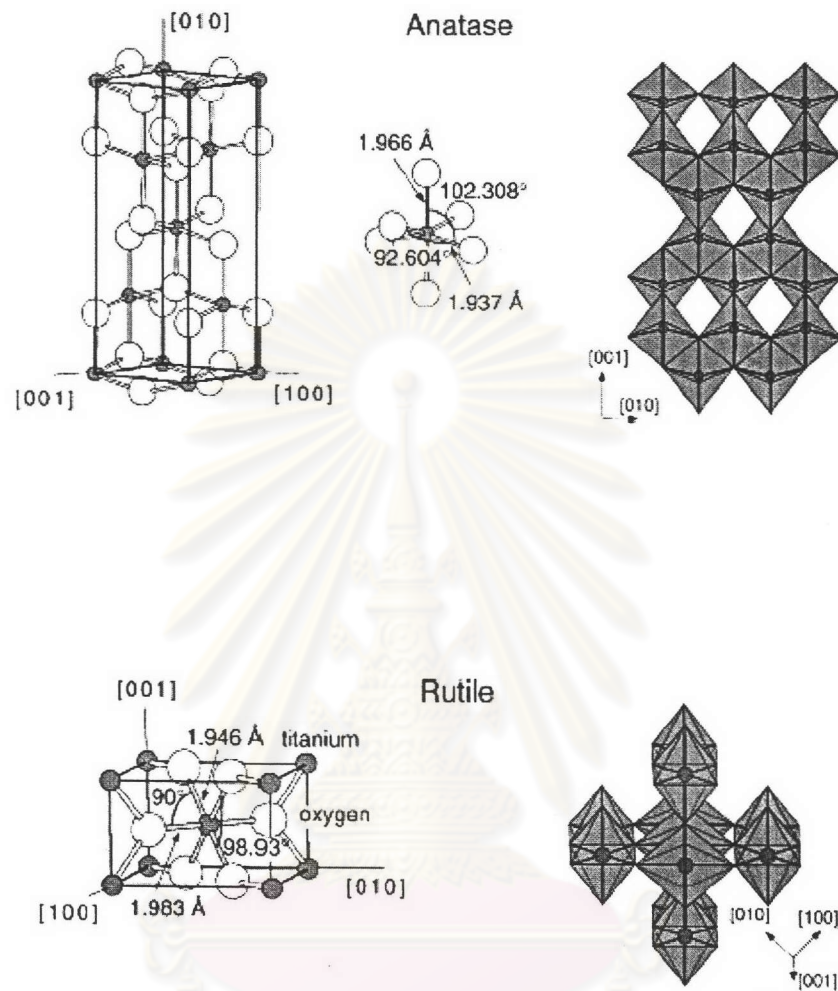| Properties	Anatase	Rutile
Crystal structure	Tetragonal	Tetragonal
Lattice constant (a, Å)	3.782	4.587
Lattice constant (c, Å)	9.502	2.953
Density (g/cm^3)	3.895	4.25
Refractive index	2.54	2.75
Band gap (eV)	3.25	3.05
Melting point (^{o}C)	Converts to rutile	1,830-1,850

ศูนย์วิทยทรัพยากร
จุฬาลงกรณ์มหาวิทยาลัย

Figure 2.1 Bulk structures of anatase and rutile. The tetragonal bulk unit cell of anatase has the dimensions, a = b = 3.782 Å, c = 9.502 Å, and the one of rutile a = b = 4.587 Å, c = 2.953 Å [7]

2.2 Development of TiO_2 photocatalyst

The studies on photocatalytic property of TiO_2 semiconductor have been conducted in the early 1970s [1]. Recently, this kind of photocatalytic material has been commercially applied to various fields of environmental cleaning. The numerous photocatalytic applications are listed in Table 2.2. Many studies suggested that TiO_2 be the most suitable material for widespread environmental applications over other oxide semiconductor photocatalysts (ZnO, Cds, GaP, Si, Fe_2O_3, and WO_3). This is possibly due to its superior photoreactivity, non-toxicity, long-term stability, strong oxidizing power, as well as cost effectiveness. Besides, the band gap energy of TiO_2 is considerably high (around 3.0-3.2 eV) that can be activated in the ultraviolet light ($\sim$ 380 nm). Noted that the band gap energy of the photocatalyst should match the energy corresponding to the light source. The band gap and wavelength of some common oxide semiconductors are shown in Table 2.3.

Table 2.2 Some selected applications of TiO$_2$ photocatalyst [9]

Property	Category	Application
Self-cleaning	Materials for residential and office buildings	Exterior tiles, kitchen and bathroom components, interior furnishings, plastic surfaces, aluminium siding, building stone and curtains, paper window blinds
	Indoor and outdoor lamps and related systems	Translucent paper for indoor lamp covers, coatings on fluorescent lamps and highway tunnel lamp cover glass
	Materials for roads	Tunnel wall, soundproofed wall, traffic signs and reflectors
	Others	Tent material, cloth for hospital garments and uniforms and spray coating for cars
Air cleaning	Indoor air cleaners	Room air cleaner, photocatalyst-equipped air conditioners and interior air cleaner for factories
	Outdoor air purifiers	Concrete for highway, roadways and footpaths and tunnel wall
Water purification	Drinking water	River water, ground water, lakes and water-storage tanks
	Others	Fish feeding tanks, drainage water and industrial wastewater
Antitumor activity	Cancer therapy	Endoscopic-like instrument
Self-sterilizing	Hospital	Floor and wall tiles of operating rooms, silicone rubber for medical catheters and hospital garments and uniforms
	Others	Public rest room, bathrooms and rat breeding rooms

Table 2.3 The band gap positions of some common semiconductor photocatalysts [10]

Semiconductor	Valence band (VB)	Conduction band (CB)	Band gap (eV)	Band gap wavelength (nm)
TiO_2	+3.1	+0.1	3.0	380
SnO_2	+4.1	+0.3	3.9	318
ZnO	+3.0	-0.2	3.2	390
ZnS	+1.4	-2.3	3.7	336
WO_3	+3.0	+0.2	2.8	443
CdS	+2.1	-0.4	2.5	497
CdSe	+1.6	-0.1	1.7	730
GaAs	+1.0	-0.4	1.4	887

2.2.1 Principle of photocatalytic reaction

The basic principle of photocatalytic reaction at the TiO_2 surface can be described as followed:

Light absorption; $\quad TiO_2 + h\nu \longrightarrow e^- + h^+$ (2.1)

Recombination reaction; $e^- + h^+ \longrightarrow heat$ (2.2)

Oxidation reaction; $\quad D\,(ads) + h^+ \longrightarrow D^+\,(ads)$ (2.3)

Reduction reaction; $\quad A\,(ads) + e^- \longrightarrow A^-\,(ads)$ (2.4)

Where;

D = Electron donor which adsorbs on the TiO_2 surface

A = Electron acceptor which adsorbs on the TiO_2 surface

Referring to Eq. 2.1, the TiO_2 photocatalyst is illuminated by light of energy equal or greater than the band gab ($h\nu \geq E_g$). Then, electrons in valence band (VB) are excited to conduction band (CB) resulting in the formation of an excited electron (e^-) - positive hole (h^+) pairs. During the reaction process, e^- - h^+ pairs may recombine on the surface or in the bulk of particles in a few nanoseconds and generates heat (Eq.2.2). Finally, the oxidation and reduction processes are introduced by the separated e^- - h^+ pairs with the pollutant molecules adsorbed on the surface, as shown in Eq. 2.3 and 2.4. Figure 2.2 illustrates the mechanism process of photocatalytic activity of TiO_2 photocatalyst, performing under UV light illumination.
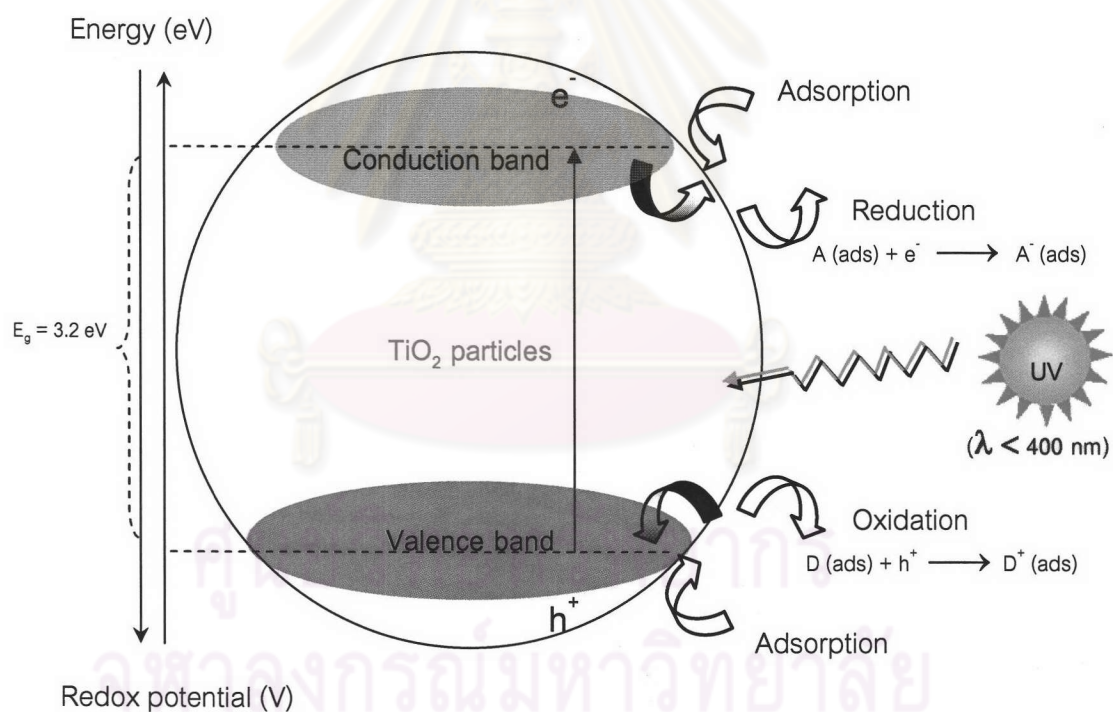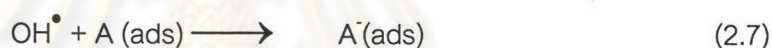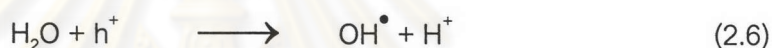

Figure 2.2 The mechanism process of photocatalytic activity of TiO_2 photocatalyst [11]

In the photocatalytic oxidation of pollutant molecules, the two possible mechanisms are involved. These are direct hole oxidation and hydroxyl radical ($OH^•$) oxidation [12]. For the direct hole oxidation, the h^+ directly reacts with the adsorbed pollutant molecules as shown in Eq. 2.3. Meanwhile, for the $OH^•$ oxidation the h+ reacts with adsorbed water or hydroxyl groups (OH^-) resulting in the forming of $OH^•$. These hydroxyl radicals have strong oxidizing power, which rapidly react with organic compounds and converts to carbon dioxide (CO_2), water (H_2O) and other inorganic matters. The $OH^•$ oxidation reactions are as the followed:

$$OH^- + h^+ \longrightarrow OH^• \tag{2.5}$$

$$H_2O + h^+ \longrightarrow OH^• + H^+ \tag{2.6}$$

$$OH^• + A\,(ads) \longrightarrow A^-(ads) \tag{2.7}$$

In addition, the formation of hydroxyl radicals is promoted by adding some electron scavengers such as oxygen molecules. It can trap electron out from the positive hole and converse to superoxide radical ion ($O_2^{•-}$). These attach to the intermediate product in the oxidation reaction, forming peroxide or hydrogen peroxide and then water [13]. The trapping electrons out from positive holes are as followed:

$$O_2 + e^- \longrightarrow O_2^{•-} \tag{2.8}$$

$$2H_2O + O_2^{•-} \longrightarrow 2H_2O_2 \tag{2.9}$$

$$H_2O_2 \longrightarrow 2OH^• \tag{2.10}$$
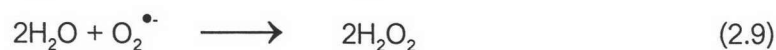
2.2.2 Parameters affecting photocalytic activity

There are many studies reporting that the photocatalytic activity of the TiO_2 greatly depends on various parameters, including crystallinity, impurity, crystal structures, particle size, as well as surface area [14 -15]. It is suggested that the anatase phase shows higher photoactivity than rutile phase. The photocatalytic difference is attributed to the difference in their energy band structures. As mentioned before, the energy band gap of anatase is 3.25 eV corresponding to the wavelength of 380 nm. Meanwhile, the band gap energy of rutile is 3.05 eV, corresponding to the wavelength of 400 nm. As shown in Figure 2.3, when electrons are excited by UV light, they move from VB to CB. Since the CB energy of anatase is higher than that of rutile and closes to the potential required to electrolytically oxidize O_2 to $O_2^{\bullet -}$, the recombination rate of e^--h^+ pairs is reduced. Moreover, it is also reported that the composite containing two phases of TiO_2 is more beneficial for suppressing the recombination of photogenerated e^- and h^+, and results in enhancing the photocatalytic activity [16].
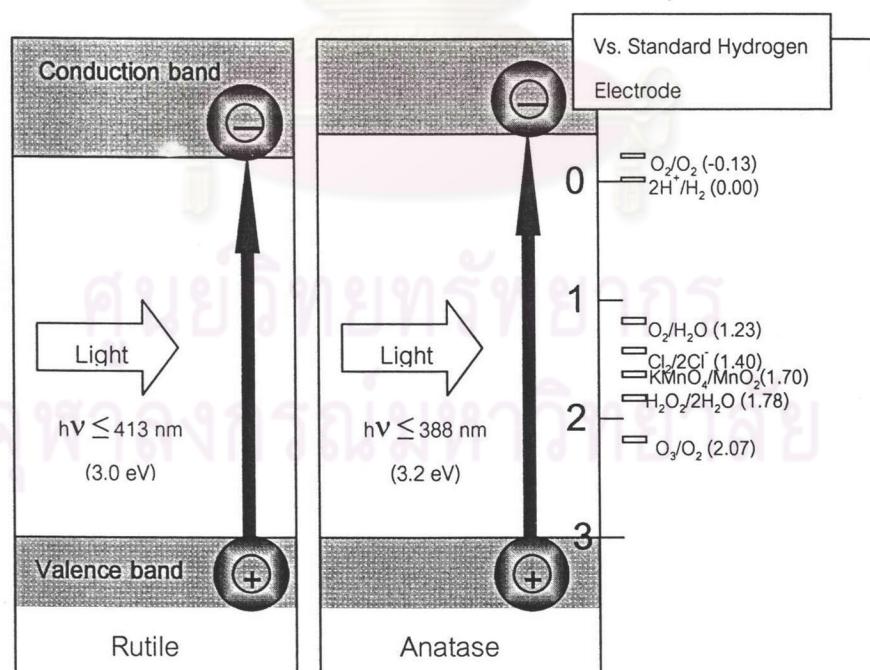

Figure 2.3 Energy diagram for TiO_2 and relevant redox potential [16]

In addition, the rate of e^--h^+ recombination is also promoted by the presence of amorphous and crystal defect in TiO_2. It generally acts as an e^--h^+ recombination center [17]. The small particle size and large surface area are considered to accelerate the rate of surface reaction of e^--h^+. Figure 2.4 shows the schematic representation of the effect of surface on the photocatalytic activity. When constant density and complete absorption of incident photons are assumed, the amount of the substrates (organics species) adsorbed on the photocatalyst will increase with increasing in surface area (decrease in particle size). Therefore, the reactions of e^--h^+ with substrates are increased [9].
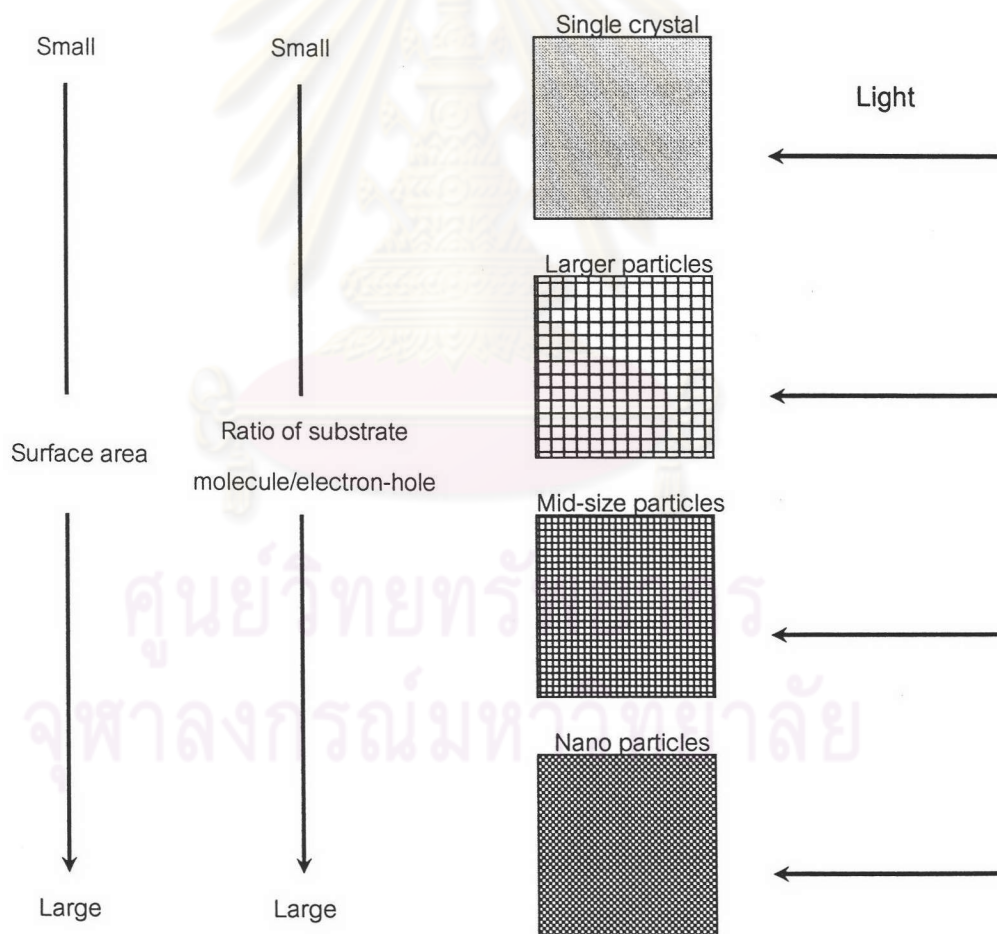
Figure 2.4 Schematic representation of the effect of surface area on the photocatalytic activity [9]
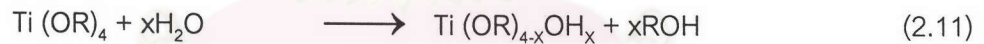
2.3 Preparation of TiO_2 photocatalyst
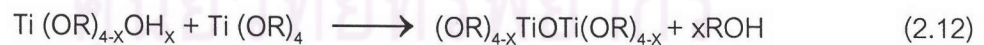
   2.3.1 Sol-gel method

It was reported that sol-gel process could be used to prepare nanosized TiO_2 photocatalyst with high surface area. It provided chemical homogeneity and possibility of deriving unique metastable structures at low temperature [18]. This method was the acceptable way of producing desired physical properties and microstructure of TiO_2, which relate to photocatalytic activity.

The preparation of TiO_2 photocatalyst by the sol-gel process involves the reaction between the titanium alkoxide and hydrolysis catalysts (H_2O, HCl, and HNO_3). In this reaction, it consists of the hydrolysis of titanium alkoxide and polycondensation as followed:

Hydrolysis reaction;

$$Ti(OR)_4 + xH_2O \longrightarrow Ti(OR)_{4-x}OH_x + xROH \qquad (2.11)$$

Polycondensation reaction;

$$Ti(OR)_{4-x}OH_x + Ti(OR)_4 \longrightarrow (OR)_{4-x}TiOTi(OR)_{4-x} + xROH \qquad (2.12)$$

Where;

      R = alkyl groups

      x = the number of terminal OH or OR groups

However, the characteristics and properties of a particular sol-gel network strongly relate to the rate of hydrolysis and polycondensation reaction. For example, the rate of hydrolysis reaction undergoes faster than condensation reaction, so that the precipitated powders are produced rather than a stable sol or gel [19]. The relative rates of these reactions not only alter the stability of sol-gel precursor, but also influence the structure and physical properties of the resulting powders. Note that the stable sol is required to obtain a good dispersion and homogeneity of TiO_2 particles on the substrate surface. The variable conditions that affect the sol-gel process included reagent concentration, nature of alkoxide, water content, type and concentration of hydrolysis catalysts, as well as aging time. Terabe and Yin [5 & 20] found that water concentration was a key factor governing the sol-gel chemistry and structural characteristics of the hydrolysis sol. High water content in the reaction medium induced a more complete hydrolysis of alkoxide, accelerating particle growth. It was reported that the use of HNO_3 as hydrolysis catalyst enhanced the crystallinity of predominant anatase while HCl reduced its amount under the same experimental condition [21-22]. Besides, fewer aggregates and finer grain size were also obtained for the sample synthesized with high HNO_3 concentration. Marukami and co-worker reported the correlation between the size of alkoxide groups and particle size of the resulting particles. This may be ascribed to the fact that the titanium alkoxide containing large alkyl groups reduced the hydrolysis rate and resulted to a fine colloidal particle [23]. Moreover, an aging time of the sol also played an important role in controlling phase composition of as-synthesized TiO_2 powders. Prolonged aging time favored the decrease of unhydrolyzed alkyl groups, resulting to the formation of rutile phase at room temerature [24].

2.3.2 Thermal treatment

In sol-gel derived process, the resulted TiO_2 powders are amorphous in nature. Since it is found to deteriorate the efficiency of photocatalytic activity, it requires further heat treatment (calcination) to promote crystallization. When calcination process is in progress, it reduces the surface area and improves the crystallinity. Thus, the preparation of TiO_2 photocatalyst with a small size, large surface area and high crystallnity requires precise control of calcination condition such as calcination temperature and time. Figure 2.5 is the whole processes for preparation of TiO_2 photocatalysts.

As mentioned previously, the calcination process frequently accelerates aggromerization and grain growth of the particle, and affects the phase transformation [26]. It was found that the amorphous-anatase transformation is observed at temerature around $350-400^{\circ}$. The anatase to rutile phase transformation has been studied for some decades by many researchers. These show that the free energy of rutile is lower than that of anatase phase at all temperatures, leading to spontaneous anatase-to-rutile transformation. The transformation is kinetically unfavorable at low temperature [27-29]. Figure 2.6 introduces the free energy of anatase-to-rutile transformation of TiO_2 as a function of temperature.

- Temperature of the
  solution-sol-gel process

- Nature of precursor
- Solvent
- Concentration of precursor

Precursor with (or without) solvent

- Chemical modification of
  the metal centre by
  reactivity changing ligands

Coordinative stabilization and chemical modification

- Hydrolysis level (molar
  water-to-alkoxide ratio)

- Acid, base, or sono-
  catalysis

Hydrolysis (formation of hydroxyl group

Polycondensation via the hydroxyl group formed

Sol, gel, precipitate, suspension

Aging

Drying

Xerogel, cryogel, aerogel
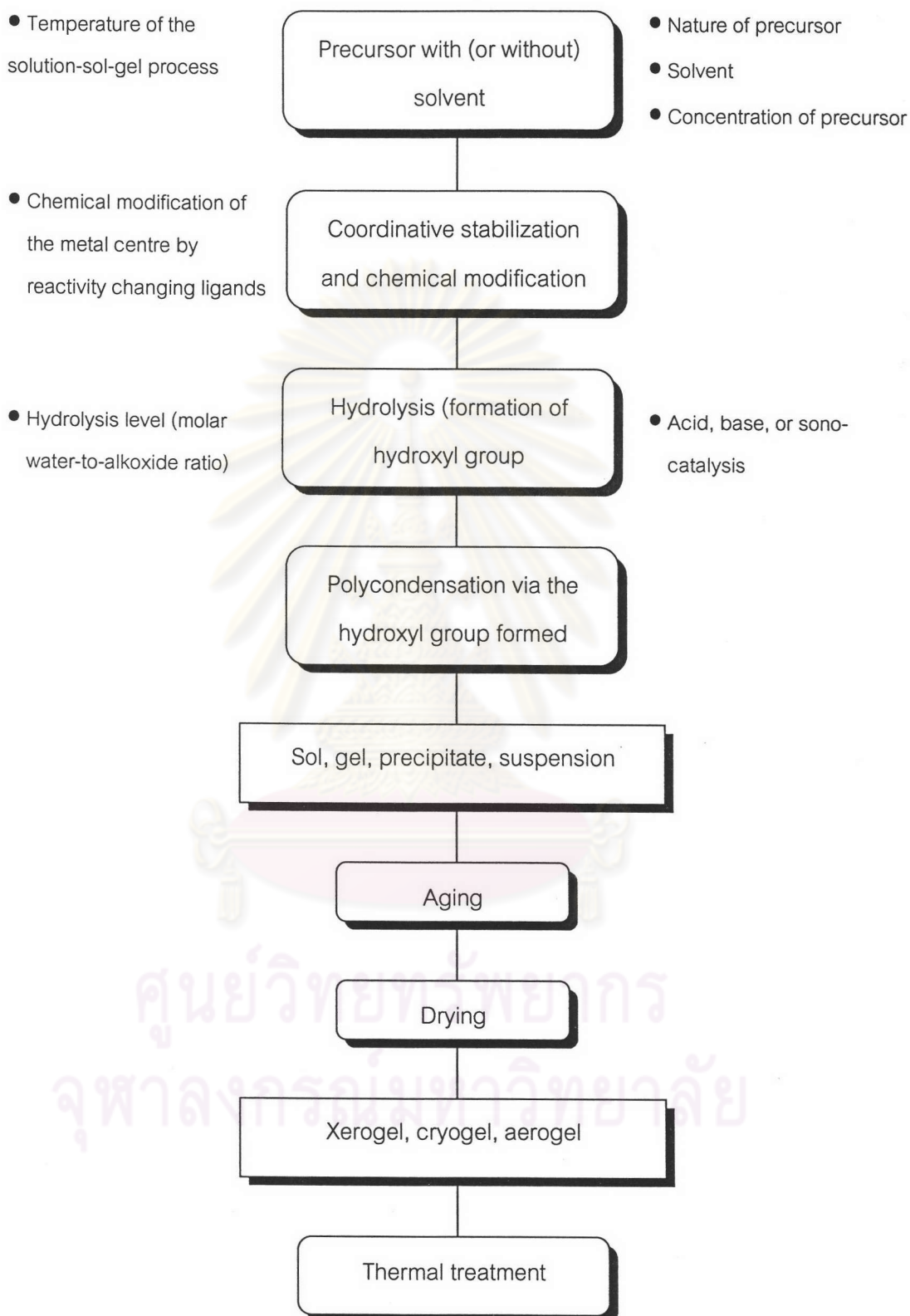
Thermal treatment

Figure 2.5 Diagram of the sol-gel process with its highly controllable tool for tailoring the properties of solid [25]
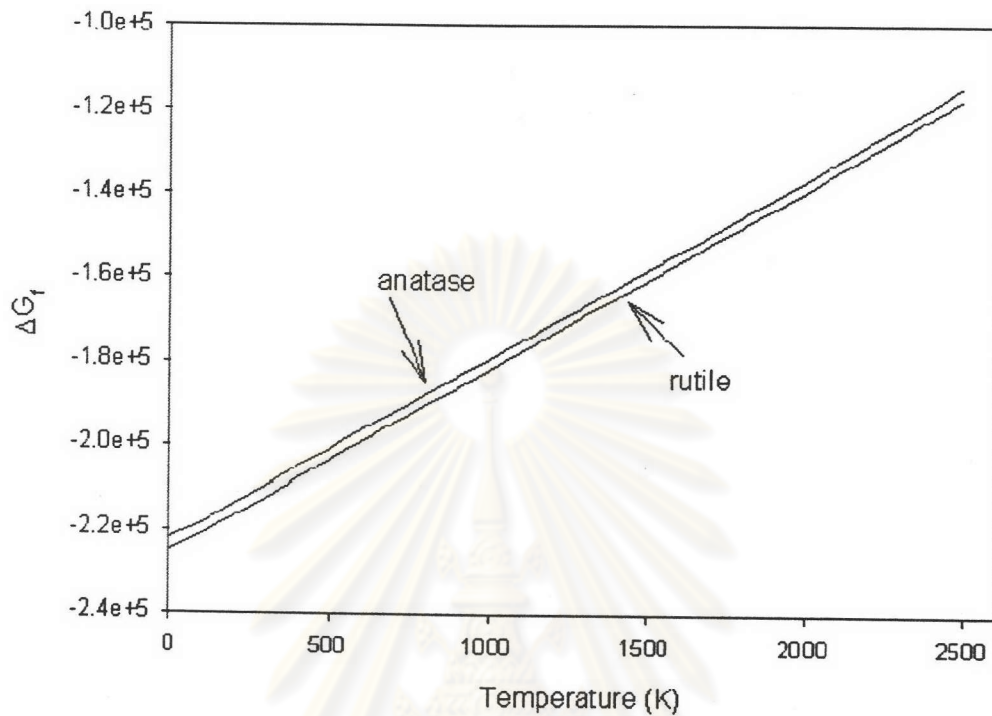
Figure 2.6 Free energy of anatase-to-rutile transformation of TiO_2 as a function of temperature [30]

According to this data, the Gibbs free energy of rutile is usually smaller than that of anatase, resulting rutile the most stable structure at all temperatures. The principle of the phase transformation generally involves the breaking and rearrangement of the Ti-O octahedra, which leads to the formation of rutile phase. Note that the anatase-rutile transformation depends on the impurities or dopants, grain size, reaction atmosphere, synthesis method, as well as synthesis condition [31-33].

2.3.3 Metal loading

Numerous studies have been performed to improve the performance of TiO_2 photocatalyst under UV illumination and to extend its light absorption into the visible region of solar spectrum. These investigations have focused on the surface and electronic modification of TiO_2 photocatalyst with metal doping. The benefits of modification of photocatalytic semiconductor system have been explained in terms of (1) inhibiting e^--h^+ recombination by increasing the charge separation (excitation of wide band gap semiconductors by UV light), (2) increasing the wavelength response range (excitation of wide band gap semiconductors by visible light).

A. Surface modification of TiO_2 photocatalysts

Figure 2.7 shows the metal-modified TiO_2 photocatalyst, performing under UV illumination. The picture schematically illustrates the metal particles covering on the TiO_2 surface. After the electrons are generated by UV irradiation, the migration of electrons to the metal particles is continuous. Then, the free holes move to the TiO_2 surface, leading to oxidizing the organic species. These result to the decrease in the e^--h^+ recombination.
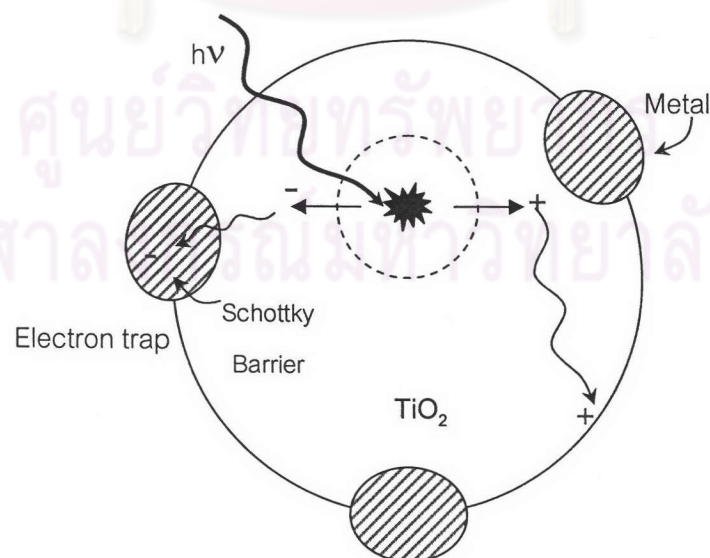

Figure 2.7 The metal-modified TiO_2 photocatalyst performing under UV illumination [34]

An enhancement of photocatalytic activity in the Pt modified TiO_2 has been studied by Phuaphromyod (1999) [35]. The Pt/TiO_2 photocatlyst showed higher activity for degradation of isopropyl alcohol than Pt or TiO_2 alone.

Zhang et. al. studied the photocatalytic decomposition of formaldehyde by using TiO_2, Pt/TiO_2, SiO_2/TiO_2, ZrO_2/TiO_2, WO_3/TiO_2 and MoO_3/TiO_2 prepared by sol-gel method. It was found that the addition of WO_3 slightly increased the photocatalytic activity, while the addition of Pt and MoO_3 decreased the activity. For SiO_2/TiO_2 and ZrO_2/TiO_2 catalysts, the highest activity was achieved at 10% SiO_2/TiO_2 and ZrO_2/TiO_2 because of its highest surface area and porosity [36].

B. Electronic modification of TiO_2 photocatalysts

Typically, TiO_2 is active only under ultraviolet (UV) light, which exists less than 10% in overall of solar light as shown in Figure 2.8
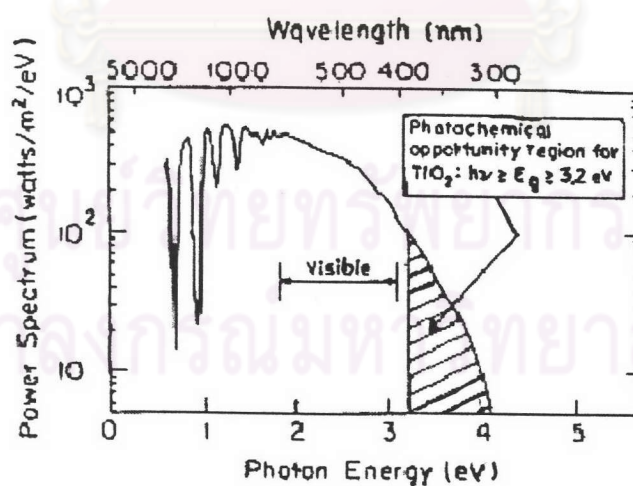

Figure 2.8 Solar spectrum at sea level with the sun zenith [34]

In order to extend the light absorption to visible region, various transition metal ions have been loaded on TiO_2 photocatalyst. An explanation of the photocatalytic activity performing under visible light illumination is shown in Figure 2.9. A small band-gap semiconductor such as CdS/TiO_2 is used to explain for this mechanism. Note that the energy of the visible light is too small to directly excite the TiO_2 particles, but it is large enough to excite an electron from the valence band across the band gap of CdS (E_g=2.5 eV) to the conduction band. According to energetic model in Figure 2.9, the photogenerated electron in the CdS valence band transfers to the conduction band of the TiO_2 particles. Meanwhile, the hole produced in the CdS valence band still remains in the CdS particle. The electrons transfer from CdS to TiO_2 increases the charge separation, resulting in the increase in the photocatalytic activity under visible light irradiation.
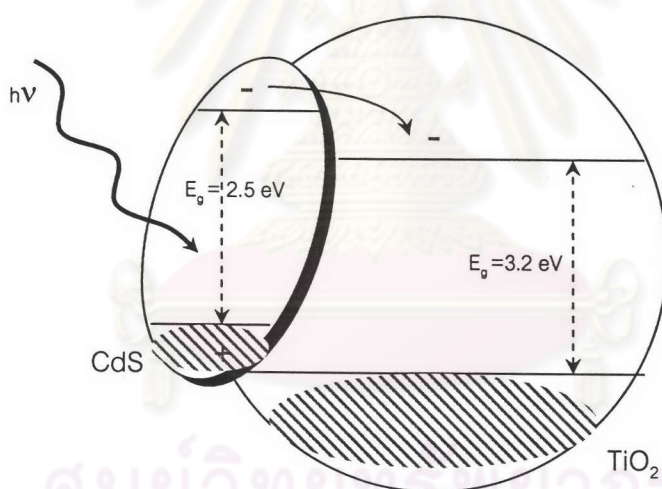

Figure 2.9 The model describing photocatalytic activity of the CdS-doped TiO_2 performing under visible light illumination [34]

Several methods have been reported for metal doping TiO_2 photocatalyst, such as ion implantation and chemical synthesis. The metal ion implantation was carried out using an ion implanter consisting of a metal ion source, mass analyzer, high voltage ion accelerator (50-200 keV), and a high vacuum pump [37]. This method was applied to modify the electronic properties of TiO_2 photocatalysts by bombarding them with high-energy metal ion. Although it overcomes a large shift in the adsorption band toward visible light region, complex operation processes are still the main problems.

On the other hand, chemical synthesis is a simple technology that does not require complicated instruments. It has been shown to product the visible-light response TiO_2 based catalyst, which possesses special catalytic properties. Methods of doping TiO_2 by chemical synthesis include mixing two powders together and then firing the product [38-39], impregnation TiO_2 powders with the metal dopant solution [40-41], as well as, the incorporatation of an active metal in the sol precursor (co-precipitation). The doping elements have usually been Cr, Fe, V, Nb, Mn, P, Si, Al, S, Ni, etc. The effectiveness of the shift in absorption band toward visible light was found to be V > Cr > Mn > Fe > Ni [9].

Scot. [1994] studied the effect of V-doped TiO_2 particles on the degradation of Chlorinated hydrocarbon. It was found that the presence of V significantly affected the crystallite size, surface area, phase transformation [42].

Zhao [1999] studied the sol-gel preparation of $Ti_{1-x}V_xO_2$ solid solution film on the conspicuous photoresponse in visible region. A series of V/TiO_2 was prepared at different V loading. It was suggested that an increase of V content promoted the anatase-rutile transformation. Further increase of V loading caused the segregation of V_2O_5 phase around TiO_2 particles, and the promotion of crystal growth and anatase-to-rutile transformation [43].

Sene [2003] studied V-doped TiO_2 thin film prepared by sol-gel method. The V loading was varied from 0.5-5.0 atomic%. For the concentration of $V \geq 1$ atomic %, it was found to have a strong effect on the surface charge of TiO_2 photocatalysts. The surface charge of V-modified TiO_2 tended to be more positive than pure TiO_2. The change in surface charge promoted an adsorption of organic species that could undergo photoelectrocatalytic oxidation. Noted that, an increase of V concentration resulted in the formation of crystalline V_2O_5. This showed that the presence of V as a dopant did not affect the band gap energy of TiO_2 [44].

Wu [2004] investigated a visible-light response, V-doped TiO_2 prepared by sol-gel method with varying % V loading (0.01-0.08 atomic %). V-doped TiO_2 was found to be mainly in anatase phase after calcination at $400^{\circ}C$. By increasing V-doping content, it promoted the particle growth and enhanced "red-shift" in the UV-visible absorption spectra. The results showed that both V^{4+} and V^{5+} co-existed in V-doped TiO_2 as a solid solution of $Ti_{1-x}V_xO_2$ could be obtained by co-precipitation of metal ion via sol-gel process. The uniformly and highly dispersed state of V^{4+}- or V^{5+}- incorporated TiO_2 photocatalyst improved its electronic properties. Therefore, the photocatalytic reaction of V-doped TiO_2 showed higher activity than pure TiO_2 under visible light irradiation [45]. This experimental result was consistent with the work of Park et. al. (2004). The V-doped TiO_2 powders formed $Ti_{1-x}V_xO_2$ solid solution possessing high photocatalytic activity under visible light radiation [46].

2.4 TiO$_2$ coating on substrates

As described previously, the high photoreactive TiO$_2$ powders are usually prepared by sol-gel method. Although it provides chemical homogeneity of final products, the yield of TiO$_2$ powders is found to be lower than other methods. This drawback can be solved by immobilizing the TiO$_2$ onto the solid supports such as glass spheres, reactor wall, fiber glass, silica gel, as well as ceramic ball. Moreover, the immobilization of TiO$_2$ in the form of thin film also provides an advantage over TiO$_2$ powder in several applications. It is used to improve the recovery of the solid after the reaction. Several studies for immobilization of the TiO$_2$ on solid supports have been reported.

Matthews [1987] studied a photooxidation of organic impurities in water by using thin film TiO$_2$ immobilized on borosilicate glass tube reactor. The tube was soaked in TiO$_2$ (P-25) suspension for several times in order to build up successive layers of TiO$_2$ inside surface of the tube. It was reported that the improvement of photocatalytic activity of salicylic acid under UV illumination was achieved by increasing the thickness of TiO$_2$ layer [47].

Paz and Luo [1995] studied the photocatalytic activity of self-cleaning TiO$_2$ coating on glass by sol-gel method. The photocatalytic films of TiO$_2$ were formed on various types of glass substrates such as soda lime glass and fused quartz. It showed that the rate of photooxidation of contaminant in soda lime glass was smaller than those in fused quartz. Moreover, the photoactivity of TiO$_2$ film on soda lime glass was lost due to the sodium ions from the glass diffuses into contacting zone of TiO$_2$ layer and form a sodium-titanium-oxygen compound [48].

Sawunyama [1998] studied the preparation and photocatalytic activity of TiO$_2$ film on glass substrates and porous alumina membranes by spin coating. A multilayered film on these two substrates was fabricated by repeating the coating cycle for eight times, i.e., spin

coating, drying at room temperature, and drying at 300°C for 10 min. It showed that all films had a sponge-like microstructure, which is crucial for a good photocatyst [49].

Fabiyi [1999] studied the photocatalytic decomposition of methylene blue by using TiO_2 coated polystyrene beads. The P-25 TiO_2 powders were simply mixed with polystyrene beads and then heated to 200°C to allow TiO_2 to adhere to the soft surface of the beads. The results showed that the coated beads have high mechanical stability as well as good photocatalytic activity. Moreover, it was found that the coated beads were easily settled out than in the form of powder [50].

Ding [2001] studied the performance of the TiO_2 film supported on various porous solid substrates such as activated carbon, γ-Alumina (Al_2O_3) and silica gel. The coating times were varied in order to obtain more uniform TiO_2 coating. It was found that among the three types of coating materials, silica gel having higher surface hydroxyl groups and surface area showed the highest activity in the photocatalytic degradation of phenol in water [51].

Kemmitt [2003] reported the preparation of TiO_2 coating on aluminium and anodized aluminium substrates by spray coating. It was suggested that the spraying technique significantly influenced the porosity of the resulting coated samples. The sample possessing higher porosity that had high surface area showed the greater photocatalytic activity [52].